VIP The following Communications have been judged by at least two referees to be "very important papers" and will be published online at www.angewandte.org soon:

Books

Highlights

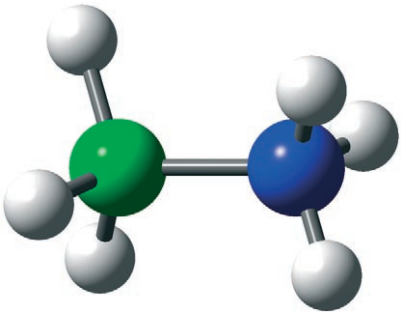

The B all and N all? Ammonia–borane (AB, H_3NBH_3) contains 19.6 weight% H, and is one of the materials currently being examined as a possible H_2 source for use in fuel cells to power automobiles. Challenges for this technology are noted, and recent advances, especially in the development of both transition-metal and acid catalysts which promote H_2 release from AB under mild conditions, are highlighted.

Hydrogen Storage

Minireviews

A multipurpose component: Owing to their size and unique properties, fullerenes, and especially C_{60}, have found applications in molecular machines, for example, as stoppers in rotaxanes. C_{60} has been introduced in molecular shuttles as an electro- and photoactive stopper that is able to induce and modulate shuttling through π–π interactions.

Molecular Machines

Contents

Reviews

An important factor in many diseases based on the deposition of amyloids is the fibrillization of peptides. Furthermore, fibril formation also promises applications in bionanotechnology: fibrillar peptide hydrogels can be made for cell scaffolds and as substrates for functional and responsive biomaterials, biosensors, and nanowires. The mechanisms and kinetics of fibril formation are discussed.

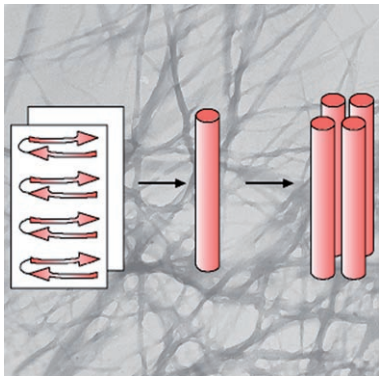

Communications

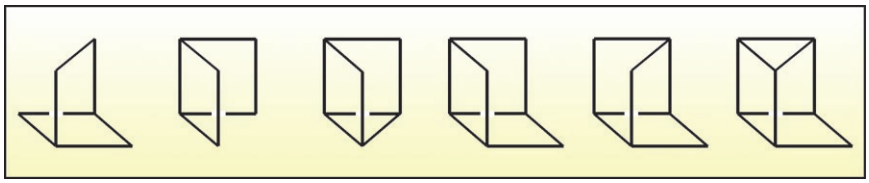

Molecular hieroglyphics: ^{29}Si COSY NMR spectroscopy reveals the fascinating and beautiful array of aqueous silicate anions that exist in dynamic equilibrium under alkaline conditions. Six of the most abundant oligomers are shown above, with each line representing a Si-O-Si siloxane linkage.

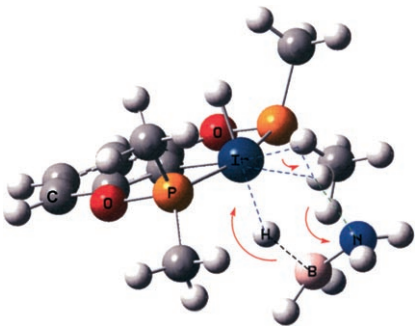

Not a bit like his brother: DFT studies show that ammonia–borane dehydrogenations by iridium pincer complexes occur by concerted hydride and proton transfer from ammonia–borane to the catalyst, not through B–H activation and subsequent β-hydride elimination from the nitrogen end, as had been suggested. Such a concerted dehydrogenation pathway does not exist for ethane, which is isoelectronic with ammonia–borane.

For the USA and Canada: ANGEWANDTE CHEMIE International Edition (ISSN 1433-7851) is published weekly by Wiley-VCH, PO Box 191161, 69451 Weinheim, Germany. Air freight and mailing in the USA by Publications Expediting Inc., 200 Meacham Ave., Elmont, NY 11003. Periodicals postage paid at Jamaica, NY 11431. US POSTMASTER: send address changes to *Angewandte Chemie*, Wiley-VCH, 111 River Street, Hoboken, NJ 07030. Annual subscription price for institutions: US$ 7225/6568 (valid for print and electronic / print or electronic delivery); for individuals who are personal members of a national chemical society prices are available on request. Postage and handling charges included. All prices are subject to local VAT/sales tax.

Proven approach to a family of antimitotics: The total synthesis of phomopsin B, an antimitotic natural product, was achieved by assembling two fragments of equal complexity in a longest linear sequence of 26 steps. The approach features two catalytic transformations that set multiple stereocenters in single steps (red and blue boxes) and a general strategy for the preparation of dehydrated amino acids (green box).

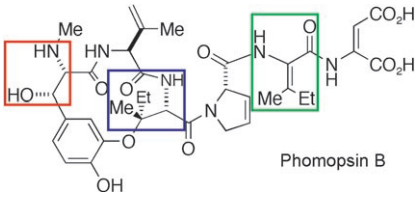

Natural Product Synthesis

Three's a crowd: Initial coordination of diethylene glycol to SmI_2 liberates THF or iodide, thus providing open coordination sites for substrates and enhancing reactivity. Concentrations of diethylene glycol that lead to coordinative saturation of SmI_2 (see structure) reduce its reactivity. Replacement of a hydroxy proton with a methyl group decreases the affinity of the chelate for SmI_2, resulting in a decrease in the reactivity of the complex.

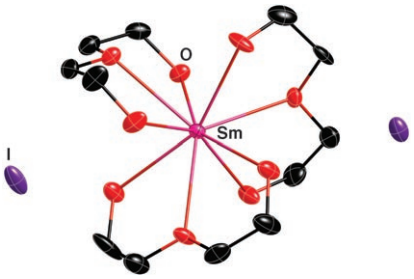

Reaction Mechanisms

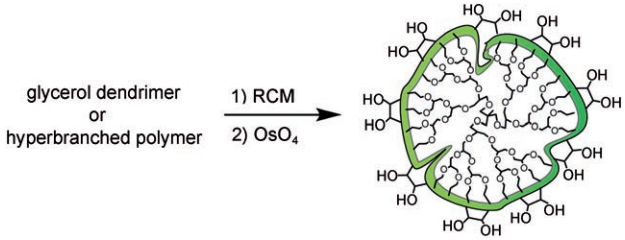

Like a big crown (ether): Cross-linked glycerol-based nanoparticles have been synthesized by ring-closing metathesis (RCM) of polyallyl glycerol dendrimers or hyperbranched polymers (see scheme). In organic solvents, the polyether nanoparticles show modest ionophoric abilities.

Organic Nanoparticles

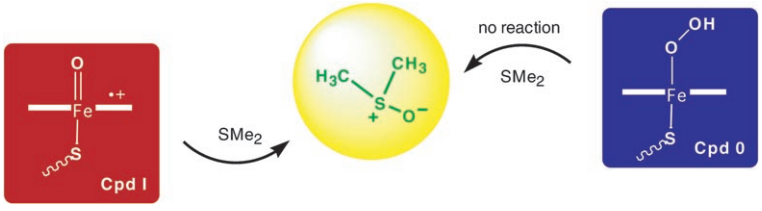

Clarifying a conundrum: The question of whether Compound I or Compound 0 (Cpd I or Cpd 0) is the reactive oxidant in the sulfoxidation of thiafatty acids by P450 is addressed by theory, which demonstrates that Cpd I leads to an extremely fast process, while Cpd 0 is at least six orders of magnitude slower. Most likely, thiafatty acids promote Cpd I formation even in the T→A mutant of $P450_{BM3}$.

P450 Sulfoxidation

Incredibly inexpensive!

Do chemistry journals really cost so much? Perhaps some do, but certainly not *Angewandte Chemie*! In 2006, an entire institution could subscribe through Wiley InterScience for about 4000 Euro and get access to 48 issues with over 1600 articles and all associated online search options, and for just 10% more, the printed issues could be included as well. For full members of the German Chemical Society (GDCh), a personal subscription cost not even 300 Euro, and student GDCh members paid less than 140 Euro, which is just under 3 Euro per issue – a price that even compares with high-circulation newsstand publications!

GDCh Gesellschaft Deutscher Chemiker

BICENTENNIAL 1807 WILEY 2007 BICENTENNIAL

service@wiley-vch.de
www.angewandte.org

WILEY-VCH

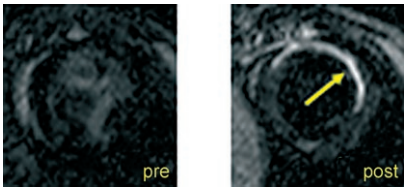

A cyclic peptide specific for type I collagen is derivatized with three {Gd(dtpa)} moieties to create a molecular MRI contrast agent for fibrosis imaging. In a mouse model of myocardial infarction (heart attack), collagen levels are elevated in the infarct zone. MRI after injection of the contrast agent selectively enhances and delineates the infarct zone (see preinjection and postinjection images); dtpa = diethylenetriaminepentaacetate.

Contrast Agents

Perfectly faceted tetrahedral 3D superlattice crystals, which are built up of 3.5-nm Ag_2S crystals, have been directly prepared through a simple one-step, two-phase reaction. The as-prepared nanocrystals assemble at the interface of water and dodecanethiol phases to form superlattice films, then break into triangular flakes, and finally stack to form tetrahedra; inset of TEM image: fast Fourier transform pattern of the superlattice (SL).

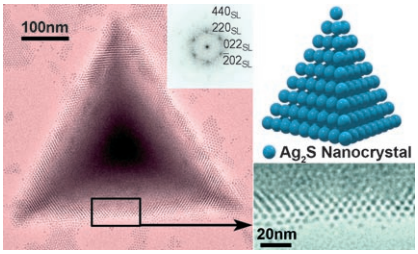

Nanostructures

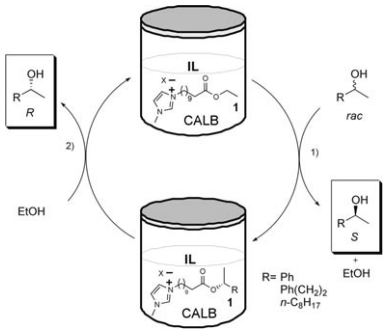

Going their different ways: A simple, robust, efficient, and reusable system for the one-pot preparative resolution and separation of *sec*-alcohols is described. The system is based on the combination of sequential enzymatic kinetic resolution (lipase B from *Candida Antarctica*, CALB) and transesterification in ionic liquids (ILs) with an ionic acylating agent **1** and removal of each enantiomer by extraction with an organic solvent.

Biocatalysis

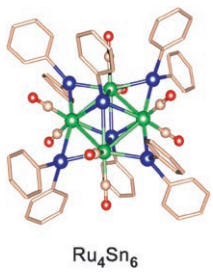

Ru_4Sn_6

Tin(n)y catalysts: Bimetallic RuSn supported nanoparticle catalysts (see picture; Ru green, Sn blue, O red), prepared from the carbonyl-cluster precursors $[Ru_4(\mu_4\text{-}SnPh)_2(\mu\text{-}SnPh_2)_{4-x}(CO)_{12-x}]$ ($x = 0, 2, 3, 4$) are shown to be active catalysts for the highly selective hydrogenation of 1,5,9-cyclododecatriene to cyclododecene under mild conditions.

Heterogeneous Hydrogenation

Contents

All lined up: Supramolecular assemblies are aligned by a convective flow in clear, nonviscous dilute solutions (see picture). The linear dichroism created by the alignment results in artifacts in circular dichroism measurements, the origins of which are explained.

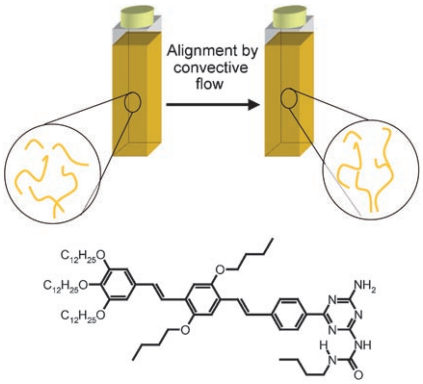

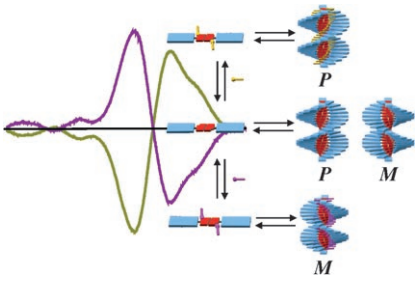

Regulating the twist: Tunable supramolecular chirality is induced in an achiral helical self-assembly (*P*, *M*; see picture) by hydrogen-bonded chiral guest molecules (yellow and purple rods). Chiroptical probing of the π-conjugated chromophore reveals the mechanistic pathways of chiral induction. "Majority rules" and "sergeant and soldiers" experiments give insight into the chiral amplification in the stacks.

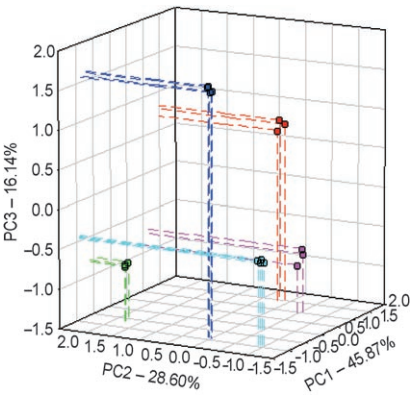

Patterning pain: Six strong-binding receptors for the decapeptide tachykinin neurotransmitter α-neurokinin were identified by screening a solid-supported library. Solution-phase studies with these six receptors metalated with three different metal salts in a 96-well plate array followed by principal component analysis showed the array's ability to recognize and discriminate substance P and α-neurokinin, as well as three similar peptides.

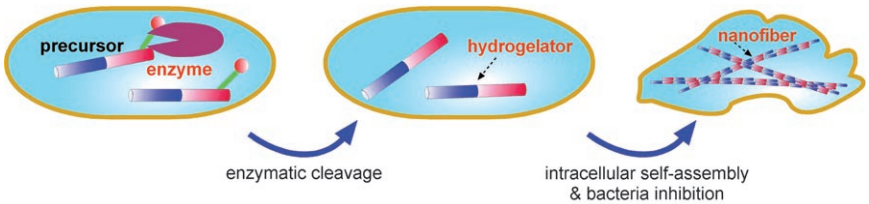

Control from within: Supramolecular hydrogelation to form nanostructures intracellularly (see picture) has been developed as a new methodology to control the fate of cells. Enzyme-regulated self-assembly of small molecules inside cells could lead to a new paradigm for managing cellular processes, understanding cellular functions, and developing new therapeutics through supramolecular chemistry.

Contents

Pushing the envelope: The calculated free energy profile for the insertion of H-ras anchor into a dimyristoyl-*sn*-glycero-3-phosphocholine bilayer shows a steeply downhill profile. The insertion into the hydrocarbon core of the ras lipids and the interfacial localization of the backbone together account for a binding free energy of about -30 kcal mol^{-1}.

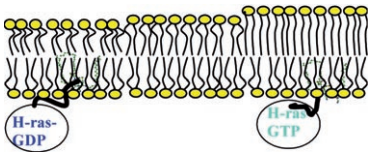

Membrane Insertion

Protection is the key: Improved resolution imaging is demonstrated with the title technique, in which a bent probe is surrounded by a 100-nm protective layer to prevent direct contact between the electrode and the sample. Submicrometer structures and characteristic chemical sites can be imaged in three different modes, as demonstrated for neurites of PC12 cells (see picture).

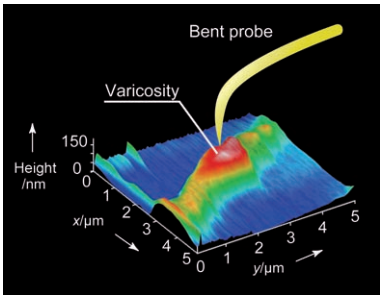

Neurite Imaging

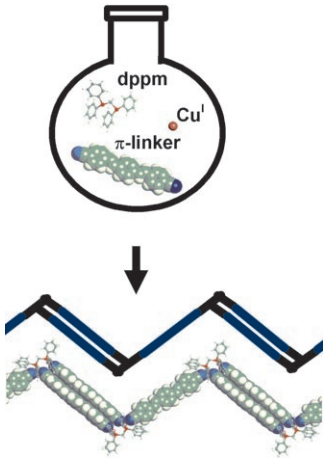

Stringing letters together: Coordination polymers (CPs) featuring unprecedented F-shaped dinuclear Cu^{I} connectors and π-stacked metallocyclophane moieties are obtained in a one-pot synthesis from their molecular components (see picture; dppm = bis(diphenylphosphino)methane; Cu pink, C gray, H white, N blue, P red). The characterization of a potential intermediate suggests that these CPs are formed through a multilevel self-assembly process.

Self-Assembly

Who is the man behind the aluminum mask? The first Group 4 Lewis acid stabilized alkylidyne (**2**; see picture) is generated by incomplete addition of trimethylaluminum across a {Ti≡C*t*Bu} moiety (**1**; PNP = [2-{P(CHMe$_2$)$_2$}-4-MeC$_6$H$_3$]$_2$N$^-$). In contrast, B(OCH$_3$)$_3$ completely adds to **1** by B–O bond cleavage to afford an unusual alkylidene. Complex **2**, a masked alkylidyne titanium compound, also ring-opens pyridine.

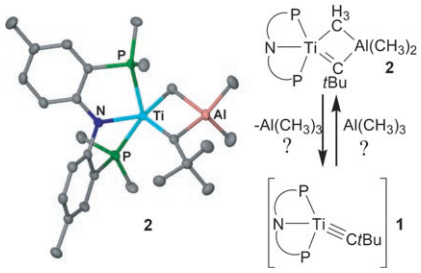

Titanium Alkylidenes

Contents

Improving inhibition: tRNA-Guanine transglycosylase (TGT) is a newly recognized target to reduce the pathogenicity of disease-causing *Shigella* bacteria. A potent family of inhibitors of this enzyme has been developed by structure-based design. Crystallographic data and pK_a analysis suggest that the aminoimidazole moiety of the central *lin*-benzoguanine scaffold is protonated and stabilization of the complexes results from charge-assisted hydrogen bonding.

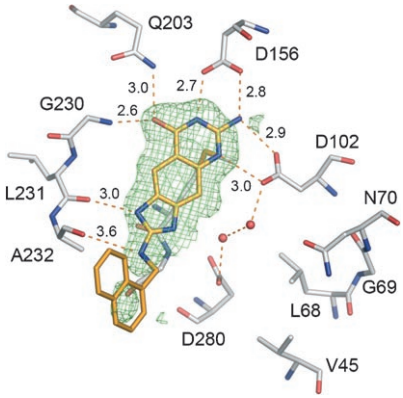

Medicinal Chemistry

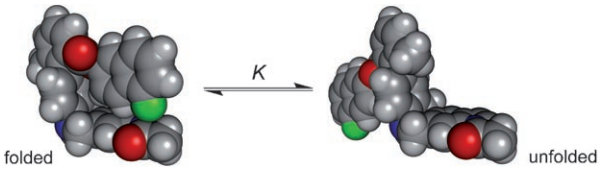

Finding the right balance: An indole-extended molecular torsion balance has the geometry for measuring a truly orthogonal noncovalent interaction between a C–F bond dipole and an amide carbonyl group (see picture, green F, red O, blue N). Employing a double-mutant cycle approach, negative interaction free enthalpies were determined. Thus orthogonal dipolar interactions can be a new tool for stabilizing protein–ligand complexes and assembling supramolecular architectures.

Supramolecular Interactions

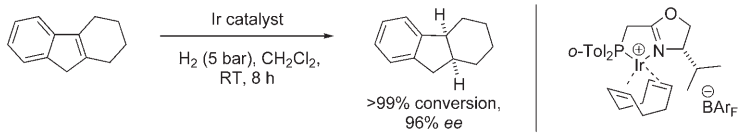

Even notoriously unreactive substrates such as tetrasubstituted unfunctionalized olefins can be hydrogenated with high efficiency and excellent enantioselectivity using readily accessible chiral Ir catalysts. In this way, two adjacent stereogenic centers can be introduced in a single step (see scheme for an example; BAr_F = tetrakis(3,5-di(trifluoromethyl)-phenyl)borate, *o*-Tol = *ortho*-tolyl).

Asymmetric Catalysis

Mixed doubles: The mixed-valent dinuclear aryltellurenyl halides $PhBr_2TeTePh$ (see picture), and RX_2TeTeR (X = ClBr, R = 2,6-$Mes_2C_6H_3$), the monomeric 2,6-$Mes_2C_6H_3TeI$, and the charge-transfer complex 2,6-$Mes_2C_6H_3TeI\cdots I_2$ are presented. The stability of H_3CEX (E = S, Se, Te; X = F, Cl, Br, I) as determined by ab initio methods are also discussed.

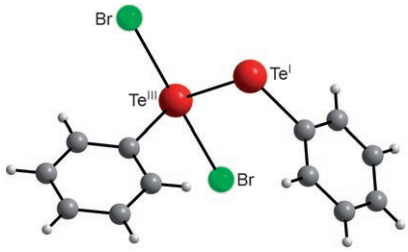

Tellurium Compounds

Contents

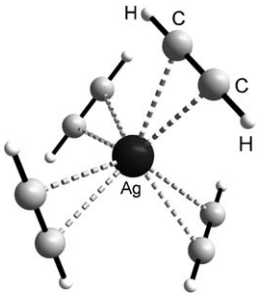

Hanging on to acetylene: The solid-state structures of the first homoleptic metal HC≡CH complexes $[M(C_2H_2)_x]^n$ (M = any metal; n, x = any number), salts of $[Ag(\eta^2\text{-}C_2H_2)_n]^+$ (n = 3,4), are described (see picture). The electronic structure of a $[Ag(\eta^2\text{-}C_2H_2)]$ model complex has been investigated by experimental charge-density studies.

Supporting information is available on the WWW (see article for access details).

A video clip is available as Supporting Information on the WWW (see article for access details).

Corrigenda

In this Communication, the structure of ligand **7** was incorrectly drawn. The correct structure is shown below.

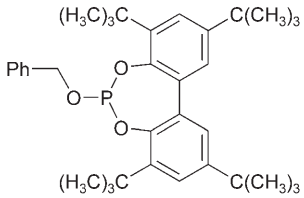

7

Mixtures of Chiral Phosphorous Acid Diesters and Achiral P Ligands in the Enantio- and Diastereoselective Hydrogenation of Ketimines

M. T. Reetz,* O. Bondarev _ **4523–4526**

Angew. Chem. Int. Ed. **2007**, *46*

DOI 10.1002/anie.200700533

In this Communication, the structure of compounds **3** and **5** was incorrectly drawn. The correct structure is shown below. The editorial office apologizes for this oversight.

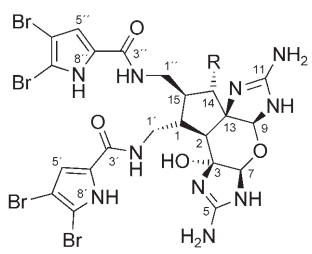

3 (R = Cl): Massadine Chloride
5 (R = OH): Massadine

Massadine Chloride: A Biosynthetic Precursor of Massadine and Stylissadine

A. Grube, S. Immel, P. S. Baran,* M. Köck* _____ **6721–6724**

Angew. Chem. Int. Ed. **2007**, *46*

DOI 10.1002/anie.200701935